Current Eye Research

ISSN: 0271-3683 (Print) 1460-2202 (Online) Journal homepage: www.tandfonline.com/journals/icey20

Keratometry and the Central Radius with Aspheric Corneal Surfaces

Achim Langenbucher, Jascha Wendelstein, Alan Cayless, Peter Hoffmann & Nóra Szentmáry

To cite this article: Achim Langenbucher, Jascha Wendelstein, Alan Cayless, Peter Hoffmann & Nóra Szentmáry (2026) Keratometry and the Central Radius with Aspheric Corneal Surfaces, Current Eye Research, 51:4, 397-403, DOI: 10.1080/02713683.2025.2596954

To link to this article: https://doi.org/10.1080/02713683.2025.2596954

Published online: 11 Dec 2025.

CURRENT EYE RESEARCH
2026, VOL. 51, NO. 4, 397–403
https://doi.org/10.1080/02713683.2025.2596954

Keratometry and the Central Radius with Aspheric Corneal Surfaces

Achim Langenbucher[a], Jascha Wendelstein[a,b,c], Alan Cayless[d], Peter Hoffmann[e] and Nóra Szentmáry[a,f]

[a]Department of Experimental Ophthalmology, Saarland University, Homburg, Germany; [b]Department of Ophthalmology, Ludwig-Maximilian University, Munich, Germany; [c]IROC AG, Institut für Refraktive und Ophthalmo-Chirurgie, Zurich, Switzerland; [d]School of Physical Sciences, The Open University, Milton Keynes, UK; [e]Augen- und Laserklinik Castrop-Rauxel, Castrop-Rauxel, Germany; [f]Department of Ophthalmology, Semmelweis-University, Budapest, Hungary

ABSTRACT

Purpose: To develop a simple concept for deriving the central corneal radius (RC) from the keratometry (K) or simulated keratometry (SimK) radius (RS) and corneal asphericity (QC), and to show the differences RC-RS based on a large dataset of measurements from a modern anterior segment tomographer.

Methods: Comparing the local slopes of surface representations with a conoid and a reference sphere at the location of a keratometry measurement (diameter KD), RC and RC-RS can be derived as a function of RS, QC and KD. The differences RC-RS were evaluated for a large dataset containing measurements from the Casia 2 tomographer made before cataract surgery.

Results: Depending on QC and KD, RC could deviate from the measured RS by up to 0.1 mm. With prolate corneas RS overestimates RC, and with oblate corneas RS underestimates RC. For example, with a typical cornea with RS = 7.7 mm and QC=-0.22 and a keratometer measuring at KD = 3 mm the central cornea is 0.0322 mm steeper (RC = 7.6678 mm) compared to keratometric measurement. Based on the dataset, the 95% confidence interval of RC-RS with KD = 3 mm was –0.0976 to +0.0265 mm.

Conclusions: For corneal representations with a conoid surface or where central corneal radius is required e.g. for paraxial calculations, the keratometric radius of curvature could easily be converted to the central radius based on corneal asphericity and the keratometric zone diameter. With large positive or negative values of QC the differences RC-RS could be clinically relevant.

ARTICLE HISTORY
Received 21 August 2025
Accepted 25 November 2025

KEYWORDS
Keratometry; central corneal radius; conoid surface model; corneal asphericity

Background

Since the invention of the first keratometer more than 100 years ago, keratometry is well established in ophthalmology for determining corneal radius of curvature or corneal power. In manual keratometry, 2 keratometer marks located at opposite positions on the same meridian are projected to the cornea reflected off the precorneal tear film and imaged to an ocular for visual inspection. The radius of curvature is derived from the height of the marks. The location where the marks are projected onto the cornea depends mostly on the radius of curvature, with the result that for a flatter cornea keratometry is measured more peripherally and for a steeper cornea it is measured more centrally.[1,2]

Automated keratometers as integrated in optical biometers or autorefractokeratometers adopt this system of corneal front surface measurements and derive corneal front surface data in the mid-periphery at 3 or more meridians. The radii and orientations of the cardinal meridians can then be extracted from the resulting 6 or more projection marks.[3]

Placido topographers use concentric mires projected to the cornea instead of distinct marks, and the image of these mires reflected off the tear film is captured by a centrally located camera. Thousands of measurement points are evaluated, and all topographers simulate the measurement strategy of a manual keratometer and provide simulated keratometry data (SimK) derived from the mid periphery in 2 orthogonal meridians.[3]

However, due to the measurement concept, we have some limitations in keratometry:

- Firstly, keratometers do not measure corneal curvature directly. Instead, keratometers measure the local slope of the surface, and this slope at the location where the marks are projected onto the cornea is converted to a corneal curvature based on certain model assumptions.[1]
- Secondly, keratometers cannot measure corneal power. In its simplest form, the cornea as a convex-concave meniscus lens has 2 refractive surfaces. However, keratometry is restricted to corneal front surface measurement, and provides no information on the corneal back surface or corneal thickness. Typically a keratometer index is used to convert corneal front surface curvature to corneal power, but such a keratometer index is based on specific model assumptions which cannot be validated by the keratometer.[1,2]

CONTACT Achim Langenbucher achim.langenbucher@uni-saarland.de Department of Experimental Ophthalmology, Saarland University, Kirrberger Str 100 Bldg. 22, 66424Homburg, Germany.

- Finally, keratometers do not measure at the central cornea. Depending on the measurement setup, keratometers typically measure in the midperiphery about 1.5 mm distant from the corneal center. In the case of an aspheric corneal surface, obtaining a representative measure for the central corneal curvature would require back-calculation of the central corneal radius based on keratometry and corneal asphericity.

The purpose of the present study was

- to develop a strategy to calculate the central corneal radius from the keratometric radius based on the corneal front surface asphericity and the keratometric measurement zone, and
- to compare the central corneal radius with the SimK radius (representing the measure of a manual keratometer) in a large measurement series from the Casia anterior segment tomographer in eyes routinely examined before cataract surgery.

Methods

Calculation strategy

Keratometry is typically measured with a setup similar to the example shown in Figure 1. In this meridional section, keratometer marks are projected onto the midperiphery of the cornea, reflected off the precorneal tearfilm and imaged in an eyepiece. In this example, telecentric imaging is used. It is clear from the drawing that what is actually measured is the local slope of the corneal surface (surface tangent shown as dashed black line and surface normal shown as dashdotted black line). Three different example surfaces are shown (sphere in blue, prolate conoid with negative asphericity in magenta, and oblate conoid with positive asphericity). These all have the same surface slope at the projection point and would therefore all give the same keratometry readings.

For simplicity, if we assume that the corneal surface is represented as a sphere or conoid, the height of the surface with respect to the apex in each case is given by

$$ZS = RS - \sqrt{RS^2 - r^2}$$

$$ZC = \frac{\frac{r^2}{RC}}{1 + \sqrt{1 - (1+QC) \cdot \frac{r^2}{RC^2}}}$$

where RS refers to the radius of curvature of the sphere, r to the radial distance to the center, RC to the central radius of curvature of the conoid, and QC to the asphericity of the conoid. The corresponding surface slopes are given by

$$ZS'(r) = \frac{r}{\sqrt{RS^2 - r^2}}$$

$$ZC'(r) = \frac{\frac{r^2}{RC}}{\sqrt{(1+QC) \cdot \frac{RC^2}{(1+QC)^2} - \frac{r^2}{(1+QC)}}}$$

Assuming that ZS' at a radial distance KD/2 is used in a keratometer to interpret the measurement in terms of a

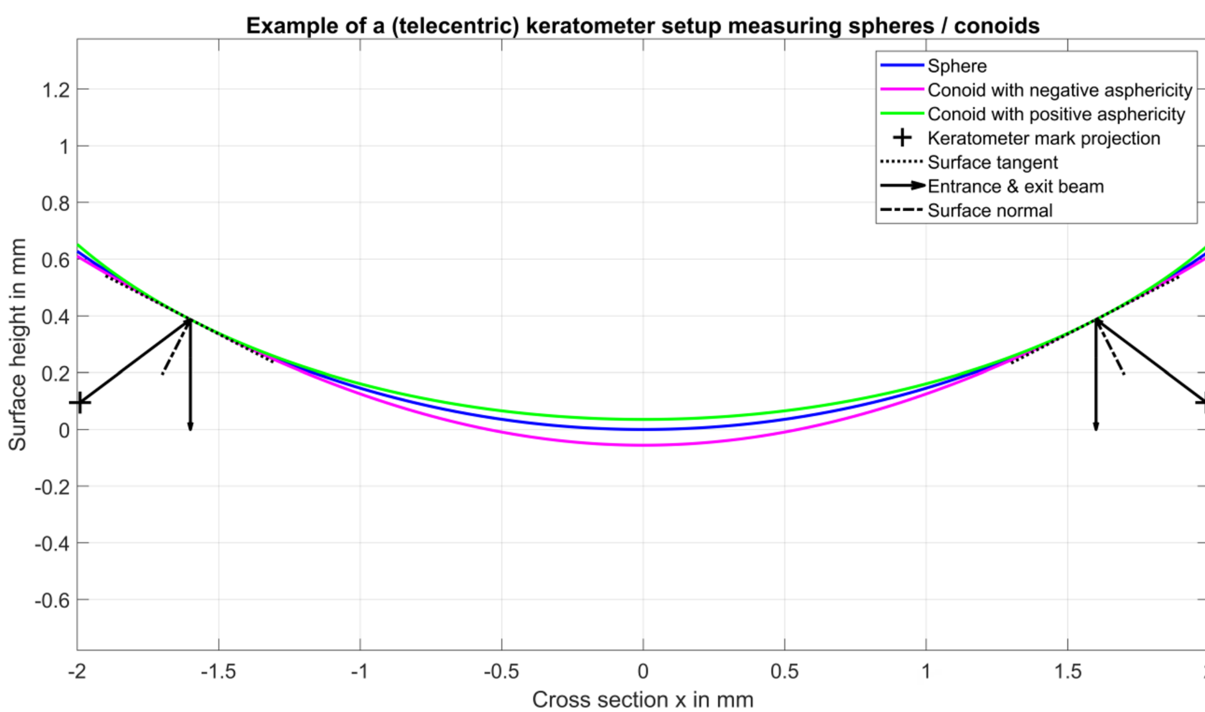

Figure 1. Schematic drawing of a keratometer measurement principle: 2 keratometer marks are projected onto the cornea, reflected off the precorneal tearfilm and imaged in an eyepiece. For this drawing we assume a telecentric imaging. With a keratometer, the local slope of the surface is measured in a Keratometric zone KD (here KD = 3.2 mm in diameter). The local slope is converted to a radius of curvature of a reference sphere (RS). However, for conic surfaces the central radius of curvature and the apex position will vary as a function of the asphericity QC.

reference sphere with radius RS, then the sphere with radius RS and the conoid with central radius RC and asphericity QC both yield the same keratometry (with keratometry zone diameter KD) when ZS'(KD/2) == ZC'(KD/2).

Solving ZS' == ZC' for RC gives:

$$RC(r) = \sqrt{\frac{RS^2 - r^2}{\left(\frac{(RS+r)\cdot(RS-r)}{RS^2 + QC\cdot r^2}\right)}}$$

When r = KD/2 this becomes:

$$RC\left(\frac{KD}{2}\right) = \sqrt{\frac{RS^2 - \frac{KD^2}{2}}{\left(\frac{\left(RS+\frac{KD}{2}\right)\cdot\left(RS-\frac{KD}{2}\right)}{RS^2 + QC\cdot\frac{KD^2}{2}}\right)}}$$

In this study, RC data and RC-RS data are evaluated for variations of KD. In addition, the height differences ZC(KD/2)-ZS(KD/2) as a measure of the surface apex displacement between the conoid and spherical surface model is recorded for variations of KD.

Dataset for our analysis

Our calculation concept is applied to clinical measurements from the Casia2 anterior segment optical coherence tomographer (Tomey GmbH, Nürnberg, Germany, software version Ver.50.5A.03). A data download containing 5224 measurements from the Augen- und Laserklinik Castrop-Rauxel, Castrop-Rauxel, Germany was assessed. The local ethics committee (Ärztekammer des Saarlandes) provided a waiver for this study (157/21). The data were filtered at the source for measurements made prior to cataract surgery. Duplicate measurements of eyes were discarded from the dataset. Where measurements of both eyes were available, one eye was selected randomly for consideration in our evaluation. After filtering, the raw export data (.CSV-format) were transferred to us in an anonymized fashion, precluding back-tracing of the patient. The anonymized dataset contained topographic measurements with SimK data (flat meridian R1 in mm oriented at an angle A1 in degrees and steep meridian R2 in mm with orientation angle A2 in degrees) and corneal front surface asphericity Qa. The CSV data were imported into MATLAB (Matlab 2024a, MathWorks, Natick, USA) for further processing. Data with quality markers QS from the Casia2 classifying the corneal front surface as other than 'OK' for the above mentioned parameters, incomplete data, and data with an ectasia screening marker other than '0%' were discarded from the dataset. The harmonic mean RS = 2·R1·R2/(R1 + R2) was derived from the radii of curvature of both cardinal meridians as a measure for the keratometric corneal radius.

Statistical analysis and data presentation

Explorative data for the differences RC - RS and ZC-ZS are listed for variations of KD (1.5 mm, 2.0 mm, 2.5 mm, 3.0 mm and 3.5 mm) in terms of the arithmetic mean, standard deviation (SD), median, and the lower and upper boundaries of the 95% confidence interval (2.5% and 97.5% quantiles). The RC and the differences RC-RS are displayed for variations of KD using boxplots showing the median (line in the box), the interquartile range (box) and the 95% confidence intervals (whiskers), and the distributions of RC-RS are visualized using a scattergraph for KD = 2.0 mm, 2.5 mm and 3.0 mm with bilinear (RS and QC) model fitted planes. A multilinear model is developed to predict RC-RS from RS, QC and KD ($(RC\text{-}RS)_{pred} \sim 1+RS+QC+KD$), where F statistics and significance level P describe the model performance compared to a constant model and R the Pearson correlation coefficient.

Results

From the $N = 5224$ measurements from the Casia2 tomographer transferred to us, a total of $N = 5131$ were used

Table 1. Explorative listing of the measured corneal radius of curvature RS and asphericity QC, and the back-calculated central corneal radius of curvature with variations of keratometric zone diameter KD (upper section), the difference RC-RS (middle), and the apex displacement ZC-ZS (lower).

Keratometry diameter KD in mm →				1.5	2.0	2.5	3.0	3.5
$N = 5131$		RS in mm	QC			RC in mm		
Measurements RS and QC and calculated RC	Mean	7.7225	−0.2195	7.7145	7.7082	7.7002	7.6903	7.6786
	SD	0.2872	0.1915	0.2882	0.2891	0.2904	0.2922	0.2947
	Median	7.7143	−0.2230	7.7044	7.6982	7.6907	7.6807	7.6677
	2.5% quantile	7.1743	−0.6554	7.1651	7.1564	7.1439	7.1329	7.1149
	97.5% quantile	8.3051	0.1330	8.3009	8.2976	8.2934	8.2834	8.2762
$N = 5131$						RC - RS in mm		
Difference measured minus calculated radius RC - RS	Mean			−0.0080	−0.0143	−0.0224	−0.0322	−0.0439
	SD			0.0070	0.0125	0.0195	0.0281	0.0383
	Median			−0.0081	−0.0144	−0.0225	−0.0325	−0.0442
	2.5% quantile			−0.0243	−0.0432	−0.0676	−0.0976	−0.1331
	97.5% quantile			0.0066	0.0118	0.0184	0.0265	0.0360
$N = 5131$						ZC − ZS in µm		
Difference measured minus calculated height ZC - ZS	Mean			0.0193	0.0613	0.1507	0.3150	0.5896
	SD			0.0170	0.0540	0.1327	0.2777	0.5202
	Median			0.0193	0.0612	0.1504	0.3141	0.5869
	2.5% quantile			−0.0154	−0.0488	−0.1195	−0.2492	−0.4644
	97.5% quantile			0.0597	0.1899	0.4676	0.9796	1.8371

Mean, SD, median, 2.5% quantile and 97.5% quantile refer to the arithmetic mean, standard deviation, median, and the lower and upper boundaries of the 95% confidence interval respectively.

after eliminating measurements with incomplete data or with a quality check other than 'OK'. Table 1 shows the descriptive data for the dataset, including RS, QC (as derived from the simulated keratometry) and RC, and also the radius difference RC-RS and the apex displacement difference ZC-ZS for variations of KD from 1.5 to 3.5 mm in steps of 0.5 mm.

Figure 2 displays the measured keratometric radius RS together with the back-calculated central corneal radius RC (left side of the graph) and the difference between RC and RS (right side of the graph) for variations of the keratometric zone KD as boxplots. The plots show that the central corneal radius systematically decreases with larger keratometric zones KD due to the typically prolate shape of the corneal front surface. However, the presence of some data points above the axis in the right-hand plot indicates that some eyes have an oblate shape, resulting in a central radius larger than the keratometric radius.

Figure 3 is a 3D scattergraph showing the difference RC-RS between the central and keratometric radii, as a

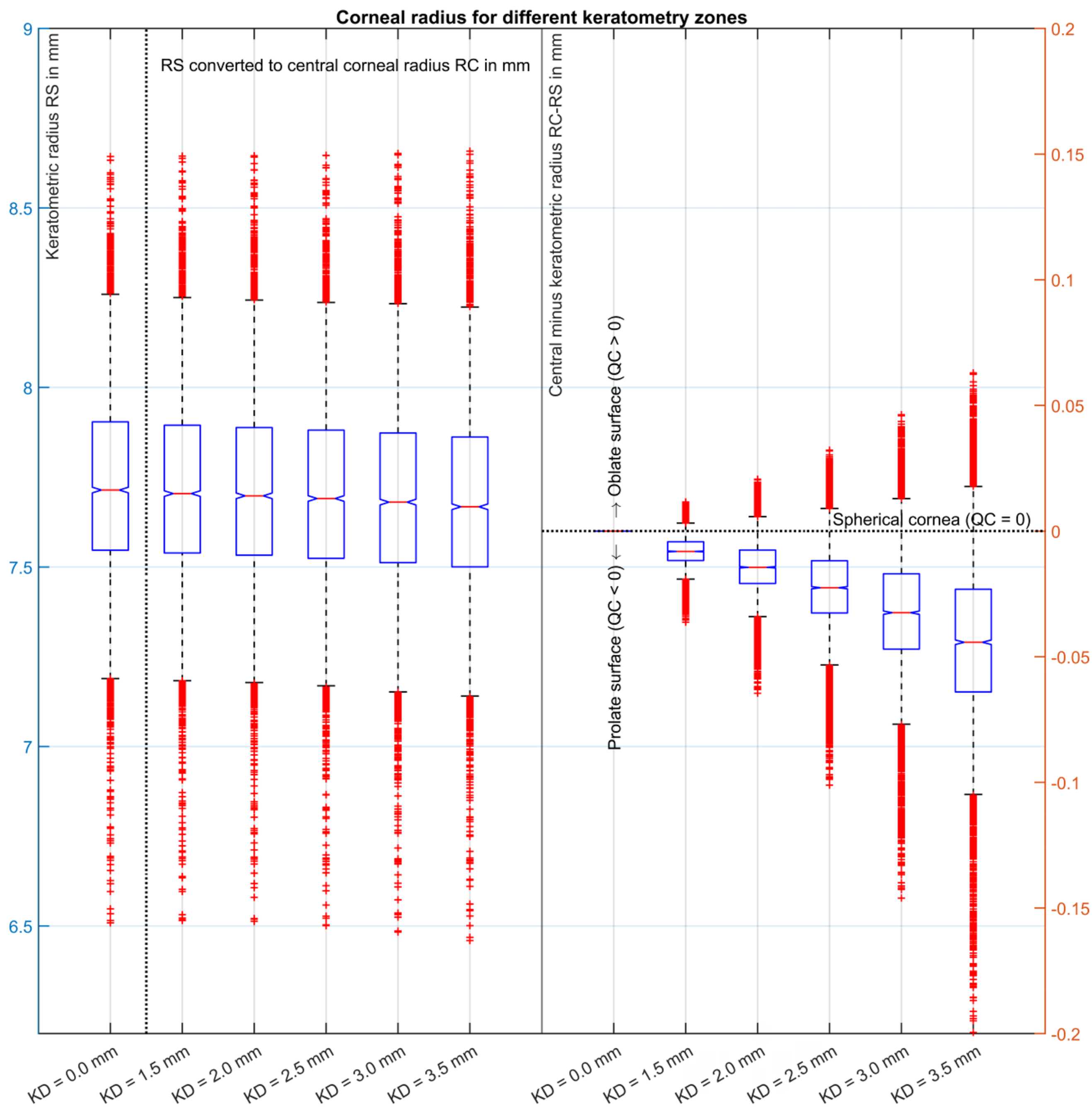

Figure 2. Boxplots for the measured keratometric radius of curvature (reference sphere RS) and the back-calculated central radius of curvature for variations of the keratometric zone diameter KD (left), and the difference between the central radius RC and the keratometric radius RS in mm (right). The red lines in the boxes indicate the median, the box margins the interquartile range, and the whiskers the 95% confidence interval. It is clear from the graph that the central corneal radius decreases systematically with larger keratometric zone diameter KD. This is explained by the mainly prolate shape of the corneal front surface. However, with oblate corneas (e.g. after myopic corneal laser vision correction) the central radius could be larger than the keratometric measurement which indicates underestimation of corneal power.

function of RS and QC with keratometric zone diameters of 2.0, 2.5 and 3.0 mm. The fitted planes show that RC deviates systematically from RS, especially for larger (mostly negative) asphericity of the corneal front surface and larger keratometric zone (KD = 3.0 mm) the.

To estimate the effects of RS and QC, we fitted a trivariate linear model to predict the difference $(RC\text{-}RS)_{pred} \sim 1+RS+QC+KD$. This model reads

$$(RC-RS)_{pred} = 2.095\cdot10^{-2} + 3.084\cdot10^{-3}\cdot RS + 1.178\cdot10^{-1}\cdot QC - 1.796\cdot10^{-2}\cdot KD$$

With a model performance of $F=2.79\cdot10^4$ and a $p<10{-}15$ as compared to a constant model ($R=0.76$). The model fit is overlaid in Figure 3 as colored planes.

Discussion

It is generally accepted in ophthalmology that keratometers measure corneal front surface curvature.[1,2] However, in practice, the system of projecting keratometer marks which are then reflected to an eyepiece actually measures local corneal slope rather than measuring the curvature directly.[3] Depending on the optical setup, keratometers typically measure in the

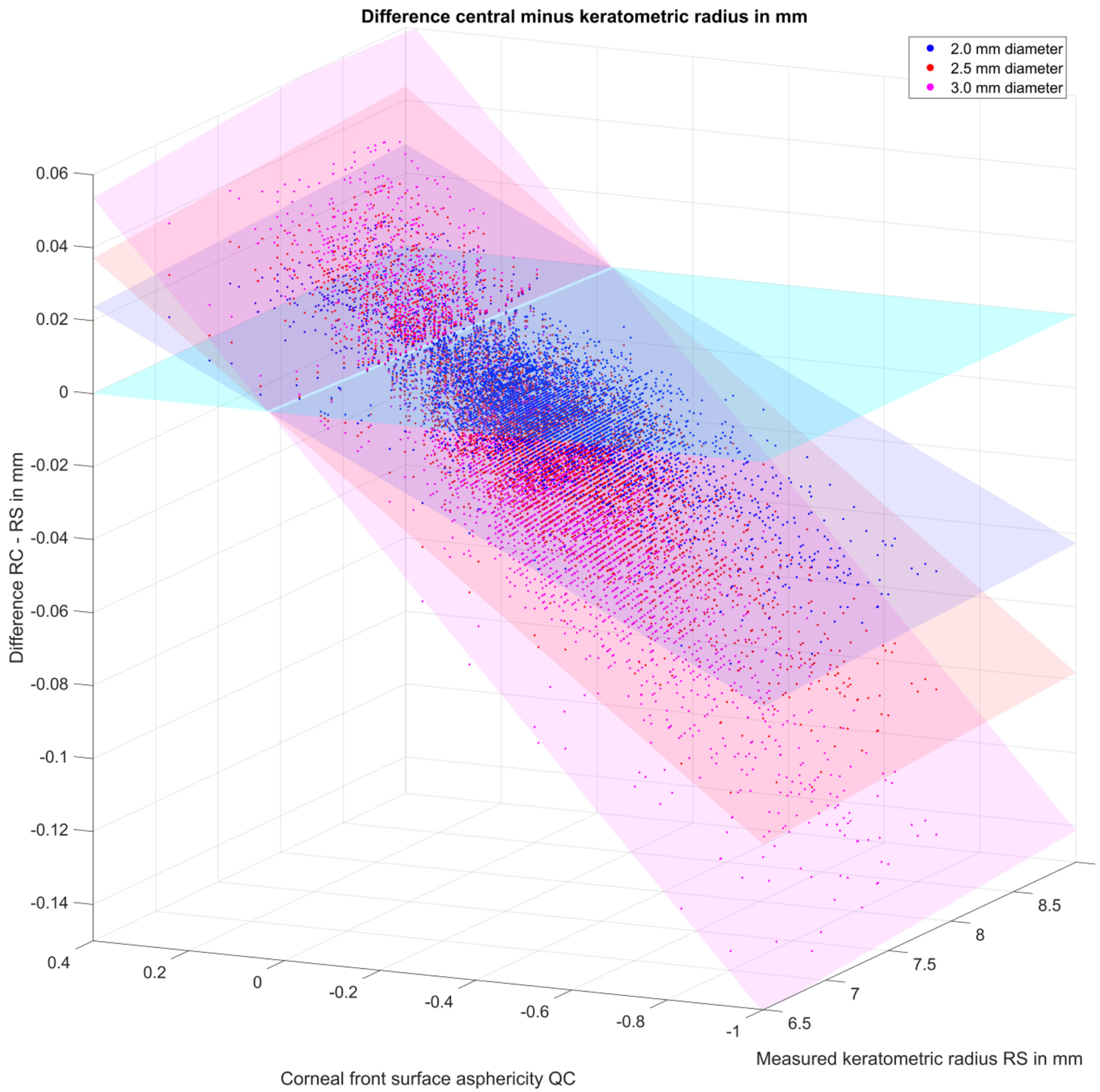

Figure 3. 3D scattergraph showing the difference between the back-calculated central corneal radius RC and the measured keratometric radius RS as a function of RS and corneal front surface asphericity QC for keratometric zone diameters 2.0 mm/2.5 mm/3.0 mm. We can easily see that RC could deviate more than 0.05 mm from RS, especially for extreme values of QC (mostly negative ones in our dataset) and with a keratometric zone diameter of KD = 3.0.

mid periphery of the cornea, and the exact location of the measurement depends on the slope. For example, with a Zeiss ophthalmometer Type H, a cornea with a 'normal' curvature of 7.7 mm is measured in a keratometry zone diameter of KD = 3.2 mm.[4] In a more curved cornea the keratometer marks are projected more centrally whereas in a flatter cornea the marks are projected more peripherally. Also, automated keratometers generally do not derive corneal curvature in the 2 principal meridians, but in 3 or more fixed meridians. The curvatures in the flat and steep meridians together with the corresponding orientation angles are then derived from the measurements in the predefined meridians. Corneal power is calculated from corneal front surface curvature using a keratometer index, which is based on a specific geometrical model for the cornea.[5,6] Since this model cannot be verified by the keratometer, this translation from curvature to power bears the risk of misinterpretation of the corneal refractive properties.[7–9] Placido topographers and most current tomographers simulate the measurement strategy of manual keratometers, and all provide so-called SimK values, which are derived from a predefined mid-peripheral zone of the cornea within a specific optical zone. In addition, they provide information about surface asphericity.[10–15]

There are several situations in ophthalmology where we represent corneal surfaces as conoids, defined in terms of a central radius of curvature together with an asphericity.[4,9,14,16–18] However, as this study shows, keratometry or SimK values from topographers or tomographers do not directly yield the exact central corneal curvature.[4,10–13,16] Instead, they provide the curvature in the mid periphery, which cannot be used to define the conoid. In this paper we have presented a simple strategy for back-calculating the central corneal radius from keratometry or SimK data together with the corneal asphericity.[6,18,19] These data could be used e.g. for raytracing through the cornea using second order surfaces to extract corneal spherical aberrations,[10,13,20] or to predict the central corneal radius[4,11,17] to perform paraxial calculations for intraocular lens power calculations.[5,21]

The results show that the keratometric radius matches the central corneal radius only for a spherical cornea. However, most corneas show some negative asphericity, resulting in a central corneal radius slightly smaller than the keratometric corneal radius.[4,11] Depending on the keratometer setup, and on the zone in which SimK values are derived in corneal topography or tomography, and the asphericity of the cornea, the keratometric corneal radius could exceed the central radius by up to 0.1 mm. For 'normal' keratometry or SimK zones of KD = 3 mm the difference between central and keratometric radius is on average -0.032 ± 0.028 mm (within a 95% confidence interval of -0.098 to $+0.027$ mm). Assuming a cornea with a keratometric radius of curvature of 7.7 mm and a Javal keratometer index of 1.3375, the 95% confidence interval for the corneal radius difference translates to a corneal power confidence interval of 337.5/(7.7-)0.0976-337.5/(7.7+0.0265) = 0.7130. This could be clinically significant in patients with non-spherical corneas, for example patients with asphericity or keratoconus, and in the prescribing of aspherical lenses, where a precise knowledge of the central corneal radius would help to ensure the best refractive outcome.

This deviation of central and keratometric radius of curvature in aspheric surfaces might also help to understand 'refractive surprises' with cataract surgery after laser vision correction or in ectatic corneas.[3] With the classical laser ablation profiles according to the Munnerlyn formula performed in the early 1990s (sometimes with high refractive corrections and small optical zone diameters), corneas were quite often shifted to an oblate configuration with a positive asphericity.[6,12,19] From Figures 2 and 3 we can clearly see that with (large) positive asphericity the central radius exceeds the keratometric radius, and as a consequence corneal power is overestimated with keratometry or SimK values. In ectatic corneal diseases we typically observe a small radius of highly negative asphericity of the corneal front surface surrounding the cone center. In these cases, and depending on the measurement strategy, we expect that keratometry will not be representative of the corneal radius of curvature, especially at the center of the cone.

However, this study has some limitations: firstly, to keep the calculations simple, we restricted the study to a stigmatic situation of the cornea. However, it is not a mathematical challenge to describe the change in corneal radius differences RC-RS separately for the flat and steep corneal meridians. Secondly, we used a large dataset of anterior segment optical coherence tomography measurements from a cataractous population to show the differences RC-RS. The results might be slightly different if measurements of a young and healthy study population were evaluated. Thirdly, we require knowledge of the corneal asphericity to translate keratometric radius to the central corneal radius. As data about asphericity is only available from topographic and tomographic measurements, this concept cannot be used together with classical keratometry. However, we feel that an approximate prediction of the difference RC-RS could also be performed using 'normal values' of corneal asphericity, which could be derived for the Casia2 e.g. from Table 1 as QC = -0.2195 ± 0.19. And finally, the reliability of asphericity measurements using topography or tomography is limited,[5,16,17] and there could be some variation in repeat measurements[7–9] or between different devices.

In conclusion, keratometers measure the local slope of the cornea at a specific distance from the center, and this slope is translated to a corneal radius of curvature assuming a spherical surface geometry. Because most corneas show some asphericity, the central corneal radius deviates systematically from the keratometric radius, and with a prolate/oblate corneal shape the central radius will be lower/higher than the keratometric radius. Especially in situations with unusual corneal asphericity, e.g. after laser vision correction procedures, the keratometric radius of curvature might not be representative and we have to calculate the central corneal radius using the surface asphericity and the keratometric zone diameter for paraxial calculations of the eye e.g. for intraocular lens power calculations before cataract surgery.

Disclosure statement

The authors report no conflicts of interest and have no proprietary interest in any of the materials mentioned in this article. The authors received no specific funding for this work.

Dr. Langenbucher reports speaker fees from Bausch & Lomb and Johnson & Johnson Vision outside the submitted work.

Dr. Wendelstein reports research grants from Carl Zeiss Meditec AG, speaker fees from Carl Zeiss Meditec AG, Alcon, Rayner, Bausch and Lomb, and Johnson & Johnson Vision outside of the submitted work.

Dr. Cayless and Dr. Szentmáry report no conflicts of interest.

Dr. Hoffmann reports speaker fees from Hoya Surgical and Johnson & Johnson and Heidelberg Engineering outside the submitted work.

Funding

This research received no specific grant from any funding agency in the public, commercial, or not-for-profit sectors.

ORCID

Achim Langenbucher http://orcid.org/0000-0001-9175-6177
Jascha Wendelstein http://orcid.org/0000-0003-4145-2559

References

1. Gurnani B, Kaur K. Keratometer. Treasure Island (FL): statPearls Publishing; 2025.
2. Sampson WG. Applied optical principles: keratometry. Ophthalmology. 1979;86(3):347–351. doi:10.1016/s0161-6420(79)35504-x.
3. Sridhar U, Tripathy K. Corneal topography. Treasure Island (FL): StatPearls Publishing; 2025.
4. Iskander DR, Collins MJ, Read SA. Extrapolation of central corneal topography into the periphery. Eye Contact Lens. 2007;33(6 Pt 1):293–299. doi:10.1097/ICL.0b013e3180319cc2.
5. Savini G, Barboni P, Carbonelli M, Hoffer KJ. Comparison of methods to measure corneal power for intraocular lens power calculation using a rotating Scheimpflug camera. J Cataract Refract Surg. 2013;39(4):598–604. doi:10.1016/j.jcrs.2012.11.022.
6. Savini G, Carbonelli M, Barboni P, Hoffer KJ. Clinical relevance of radius of curvature error in corneal power measurements after excimer laser surgery. J Cataract Refract Surg. 2010;36(1):82–86. doi:10.1016/j.jcrs.2009.07.038.
7. Langenbucher A, Szentmáry N, Cayless A, Al Karam M, Seiler TG, Wendelstein J. Repeatability of corneal curvature with the MS-39 anterior segment tomographer in a cataractous population. PLoS One. 2025;20(7):e0327863. doi:10.1371/journal.pone.0327863.
8. Langenbucher A, Szentmáry N, Cayless A, Münninghoff L, Wylegala A, Wendelstein J, Hoffmann P. Bootstrapping of corneal optical coherence tomography data to investigate conic fit robustness. J Clin Med. 2023;12(10):3522. doi:10.3390/jcm12103522.
9. Langenbucher A, Viestenz A, Seitz B. Conoidal fitting of corneal topography height data after excimer laser penetrating keratoplasty. J Refract Surg. 2002;18(1):63–71. doi:10.3928/1081-597X-20020101-10.
10. Calossi A. Corneal asphericity and spherical aberration. J Refract Surg. 2007;23(5):505–514. doi:10.3928/1081-597X-20070501-15.
11. Davis WR, Raasch TW, Mitchell GL, Mutti DO, Zadnik K. Corneal asphericity and apical curvature in children: a cross-sectional and longitudinal evaluation. Invest Ophthalmol Vis Sci. 2005;46(6):1899–1906. doi:10.1167/iovs.04-0558.
12. Gatinel D, Hoang-Xuan T, Azar DT. Determination of corneal asphericity after myopia surgery with the excimer laser: a mathematical model. Invest Ophthalmol Vis Sci. 2001;42(8):1736–1742.
13. Langenbucher A, Hoffmann P, Cayless A, Wendelstein J, Szentmáry N. Evaluation of corneal power from an AS-OCT thick lens model and ray tracing: reliability of the keratometer index. J Cataract Refract Surg. 2024;50(4):360–368. doi:10.1097/j.jcrs.0000000000001363.
14. Navarro R, González L, Hernández JL. Optics of the average normal cornea from general and canonical representations of its surface topography. J Opt Soc Am A Opt Image Sci Vis. 2006;23(2):219–232. doi:10.1364/josaa.23.000219.
15. Navarro R, Rozema JJ, Emamian MH, Hashemi H, Fotouhi A. Average biometry of the cornea in a large population of Iranian school children. J Opt Soc Am A Opt Image Sci Vis. 2019;36(4):B85–B92. doi:10.1364/JOSAA.36.000B85.
16. Gatinel D, Haouat M, Hoang-Xuan T. Etude des paramètres permettant la description mathématique de l'asphéricite cornéenne [A review of mathematical descriptors of corneal asphericity]. J Fr Ophtalmol. 2002;25(1):81–90.
17. Janunts E, Kannengießer M, Langenbucher A. Parametric fitting of corneal height data to a biconic surface. Z Med Phys. 2015;25(1):25–35. doi:10.1016/j.zemedi.2014.02.005.
18. Langenbucher A, Seitz B, Naumann GO. Three-axis ellipsoidal fitting of videokeratoscopic height data after penetrating keratoplasty. Curr Eye Res. 2002;24(6):422–429. doi:10.1076/ceyr.24.6.422.8597.
19. Gatinel D, Malet J, Hoang-Xuan T, Azar DT. Corneal asphericity change after excimer laser hyperopic surgery: theoretical effects on corneal profiles and corresponding Zernike expansions. Invest Ophthalmol Vis Sci. 2004;45(5):1349–1359. doi:10.1167/iovs.03-0753.
20. Nieto-Bona A, Lorente-Velázquez A, Mòntes-Micó R. Relationship between anterior corneal asphericity and refractive variables. Graefes Arch Clin Exp Ophthalmol. 2009;247(6):815–820. doi:10.1007/s00417-008-1013-2.
21. Langenbucher A, Schröder S, Cayless A, Eppig T. Aberration-free intraocular lenses - What does this really mean? Z Med Phys. 2017;27(3):255–259. doi:10.1016/j.zemedi.2017.03.003.